

## Supporting Information for

# Proton conductivity of imidazole entrapped in microporous molecular sieves

Aldona Jankowska,<sup>†\*</sup> Alina Zalewska,<sup>†</sup> Aleksandra Skalska,<sup>†</sup> Adam Ostrowski<sup>‡</sup> and Stanisław Kowalak<sup>†</sup>

<sup>†</sup>Adam Mickiewicz University, Faculty of Chemistry, Poznań, Poland

<sup>‡</sup>Institute of Molecular Physics, Polish Academy of Science, Poznań Poland

### Preparation:

1. Impregnation, evaporation, immersion of molecular sieves (KL, NaY, AIPO-5)

Zeolite matrices (KL, NaY) were at first transformed into H-forms by means of ion exchange procedure (via ammonium forms). The matrices were usually thermally activated before the imidazole introduction in order to remove the adsorbed compounds (i.e. water or remnants of other solvents). Imidazole (Sigma Aldrich) was used for composite preparation without further purification. Impregnation of matrices was always conducted with chloroform solution. The powder of thermally activated molecular sieves was immersed into the Him solution and stirred in closed bottle for 12 h at room temperature. Then chloroform was slowly evaporated at 323 K. This procedure enabled to introduce a controllable content of Him. The introduction of Him into matrices by vaporization in a stream of carrier gas (N<sub>2</sub>) was carried out at (403 K) in glass tube, where the vessels with imidazole and with matrix were placed. Some samples were obtained by immersion of matrices in molten Him, and then by evaporation of its excess (403 K).

2. Encapsulation - *building of a bottle around the ship (AIPO-LAU)*

We modified the traditional synthesis of AIPO-20 material<sup>1</sup> by replacing a certain fraction or whole conventional structure directing agent (e.g. TMAOH) with imidazole. Since imidazole and its derivatives are known as structure directing agents it was feasible that Him could be introduced into some molecular sieves (particularly those of narrow pore system) upon the crystallization. Contrary to the conventional hydrothermal procedure the imidazole would not be removed from the resulting product after completed crystallization. Being accommodated inside the formed matrix it could act as a proton carrier. Tetramethylammonium hydroxide (TMAOH) is usually used as template agent for synthesis of AIPO-20 (with SOD structure).

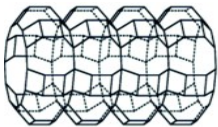
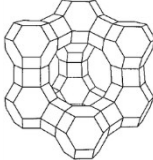
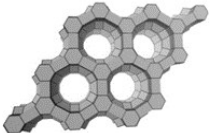
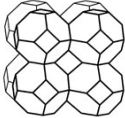
3. Encapsulation - *building of a ship inside the bottle*

Synthesis of the imidazole inside the cages of AIPO-20 (SOD) was conducted according to published recipe<sup>2</sup>, but the mixture of substrates: glyoxal (2 ml), formaldehyde (1.3ml) and water (15 ml) was

supplemented with the powder of AIPO-20 (1.35 g). The mixture was magnetically stirred in a round bottom flask for 30 minutes and pH was adjusted up to value 3.5 by means of  $\text{NH}_4\text{Cl}$  and aqueous ammonia. Then the mixture was heated at  $95^\circ\text{C}$  for 1.5 h. KOH solution was added at the end to attain pH 10 and the resulting product was separated by centrifugation. Regarding a low yield of synthesis the procedure was repeated (with the same matrix) several times.

## Characterization:

Table S1. The characteristics of prepared molecular sieves.<sup>3</sup>

| Matrix<br>[Refcode]        | Structure  | Composition  | Pore<br>characterization                            |
|----------------------------|--|--|---|
| Zeolite L<br>[01-076-9100] | LTL<br>   | The aluminosilicate with a 1D-channel structure.                 | $d_A = 7.1 \text{ \AA}$<br>$d_p = 13 \text{ \AA}$   |
| Zeolite Y<br>[01-078-6970] | FAU<br>   | The aluminosilicate with a small sodalite cages and super cages. | $d_A = 6.7 \text{ \AA}$<br>$d_p = 11.9 \text{ \AA}$ |
| AIPO-5<br>[04-012-4440]    | AFI<br>  | The aluminophosphate with a 1D-channel structure.                | $d_A = d_p = 7.3 \text{ \AA}$                       |
| AIPO-20<br>[00-043-0569]   | SOD<br> | The aluminophosphate with a small sodalite cages                 | $d_A = 2.1 \text{ \AA}$<br>$d_p = 6.2 \text{ \AA}$  |

where:  $d_A$  is the pore limiting diameter and  $d_p$  is the largest cavity diameter.

## Powder X-Ray Diffraction

One way of encapsulation comprised a hydrothermal crystallization of the matrix from initial mixtures, supplemented with Him (*building of a bottle around the ship*). A small admixture of Him into the gel usually did not affect the crystallization route, but the higher content could direct a synthesis towards other crystalline structures, sometimes quite novel ones. As shown in Fig. S1 the original initial mixture led to the SOD structure, so did the mixture with small admixture of Him (0.7 wt. %). The sample obtained from the gel containing 3.8 wt.% presents the SOD structure markedly contaminated with other structures. The product crystallized with Him as exclusive templating agent exhibits the LAU structure.

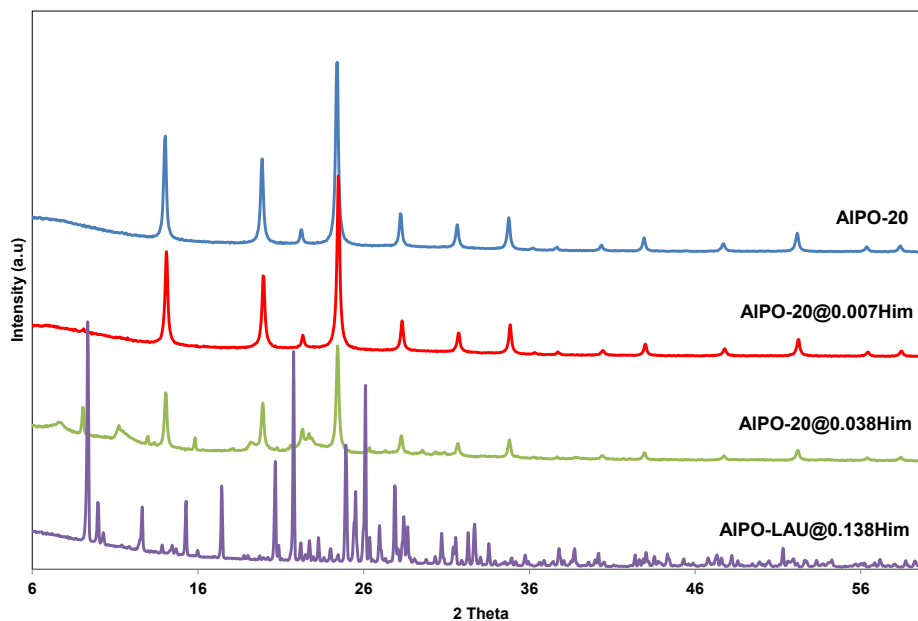


Fig. S1. PXRD patterns of selected samples.

The PXRD patterns of the composites obtained by impregnation of zeolites with the imidazole do not indicate any noticeable differences in the matrix structure, although some intensity decrease and small shift of reflections (insert) towards lower angles is seen. The shift can result from some extension of cell parameter due to accommodation of imidazole inside the matrix inner voids. The reflections assigned to imidazole (indicated with \*) appear only for the samples overloaded with Him (e.g. HY@0.314Him).

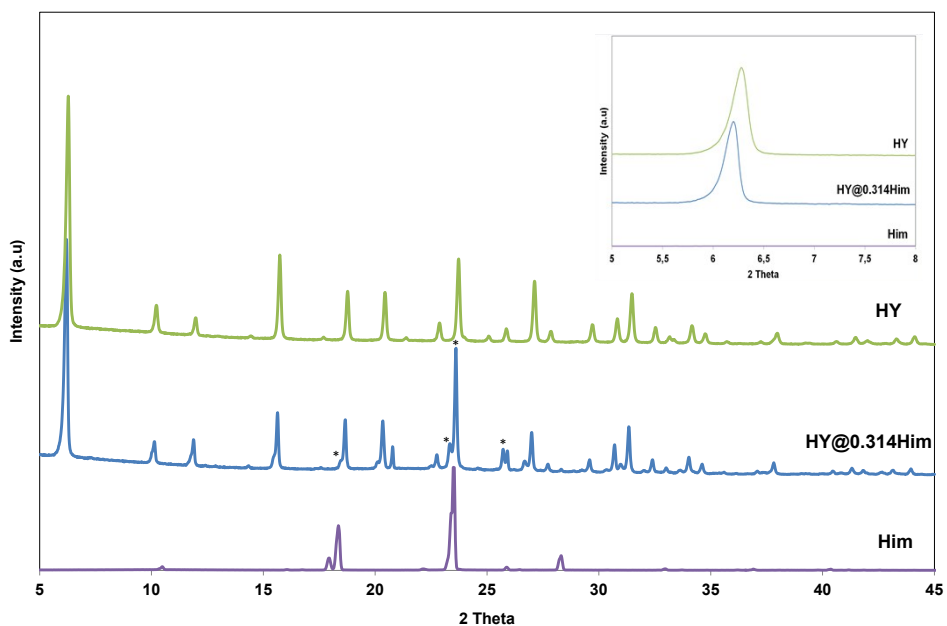


Fig. S2. PXRD patterns of zeolite HY, composite, HY@0.314Him and for pristine imidazole.

PXRD patterns were recorded with Bruker D8 Advance diffractometer with Cu-K $\alpha$  radiation ( $\lambda=1.54056$  Å).

## Thermogravimetric analyses

The thermal behavior of the samples was followed by thermal and thermogravimetric analyses (TG and DTA) in air (with heating rate of 10 °C/min) using SETARAM SETSYS 12 equipment.

The results of the thermogravimetric measurements (Fig. S3) allow to explain the nature of thermal effects in the composites in comparison to these recorded for the matrix and for the pristine Him.

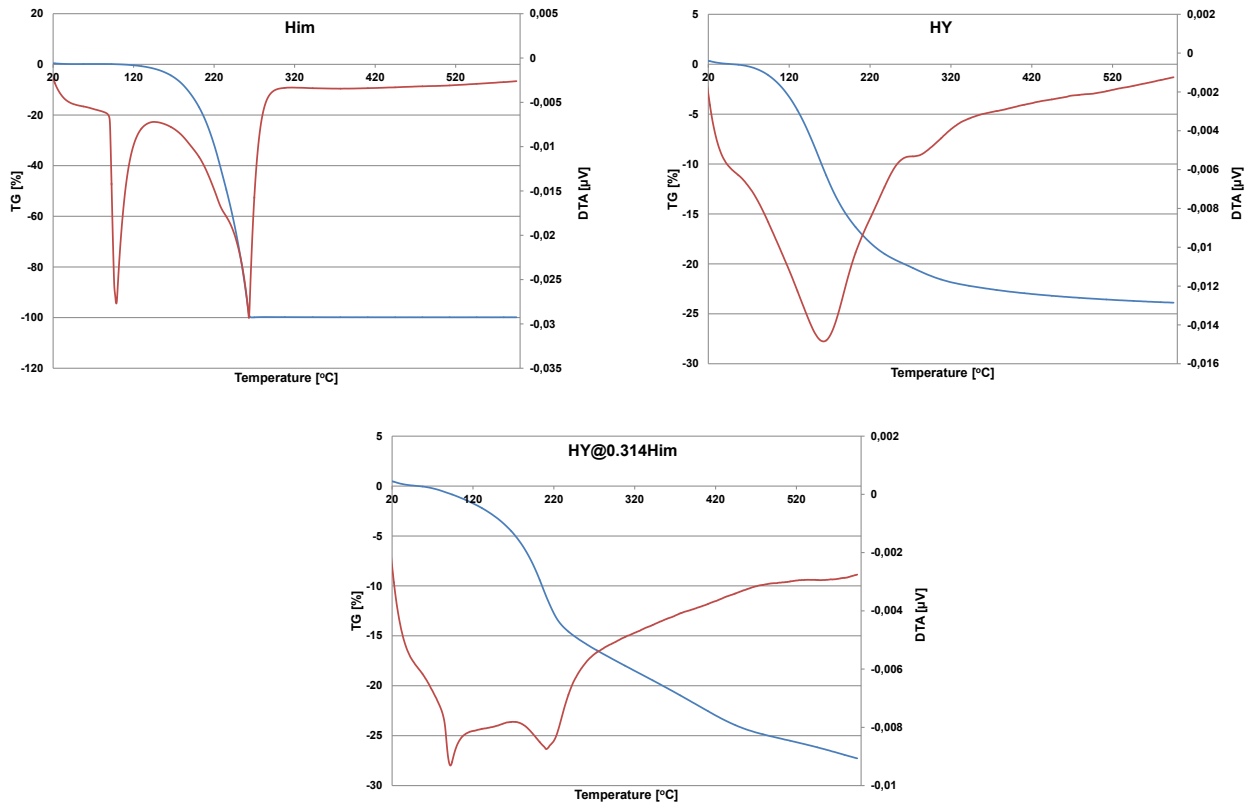


Fig. S3. Results of thermal analyses of indicated samples (pristine Him, zeolite matrix HY, composite HY@0.314Him).

## Elemental analyses

The analyzes was performed on the apparatus Elementar model Vario EL III.

Table S2. The results of the elemental analysis performed for the selected composites.

| Composite         | %N     | %C      |
|-------------------|--------|---------|
| HY@0.314Him       | 12.922 | 17.1678 |
| HY@0.284Him       | 11.684 | 15.373  |
| HY@0.242Him       | 9.959  | 13.054  |
| HY@0.158Him       | 6.502  | 8.527   |
| HL@0.202Him       | 8.313  | 10.975  |
| HL@0.171Him       | 7.037  | 9.108   |
| AIPO-5@0.175Him   | 7.202  | 9.308   |
| AIPO-LAU@0.138Him | 5.678  | 7.544   |

The estimated contents of hydrogen was usually higher than suggests the imidazole stoichiometry, which resulted from contribution of acidic OH groups in zeolites as well as from the presence of some adsorbed water. Therefore we decided to omit these data in the Table.

## Impedance Spectroscopy:

The conductivity measurement was performed by means of impedance spectroscopy (IS) in the thermo-programmed (1 K/min) heating and cooling modes in the range 300-400 K. The samples were prepared by sandwiching the respective powder in Teflon container (inner diameter 8 mm and 1.2 - 1.6 mm thickness) between two electrodes. Then the samples were placed in home-made cell in a nitrogen environment and conductivity measurements were carried out with 4284A Hewlett Packard (20 Hz - 1 MHz) Precision LCR Meters. The temperature was controlled and stabilized with the LakeShore 340 Temperature Controller.

## Nyquist diagrams

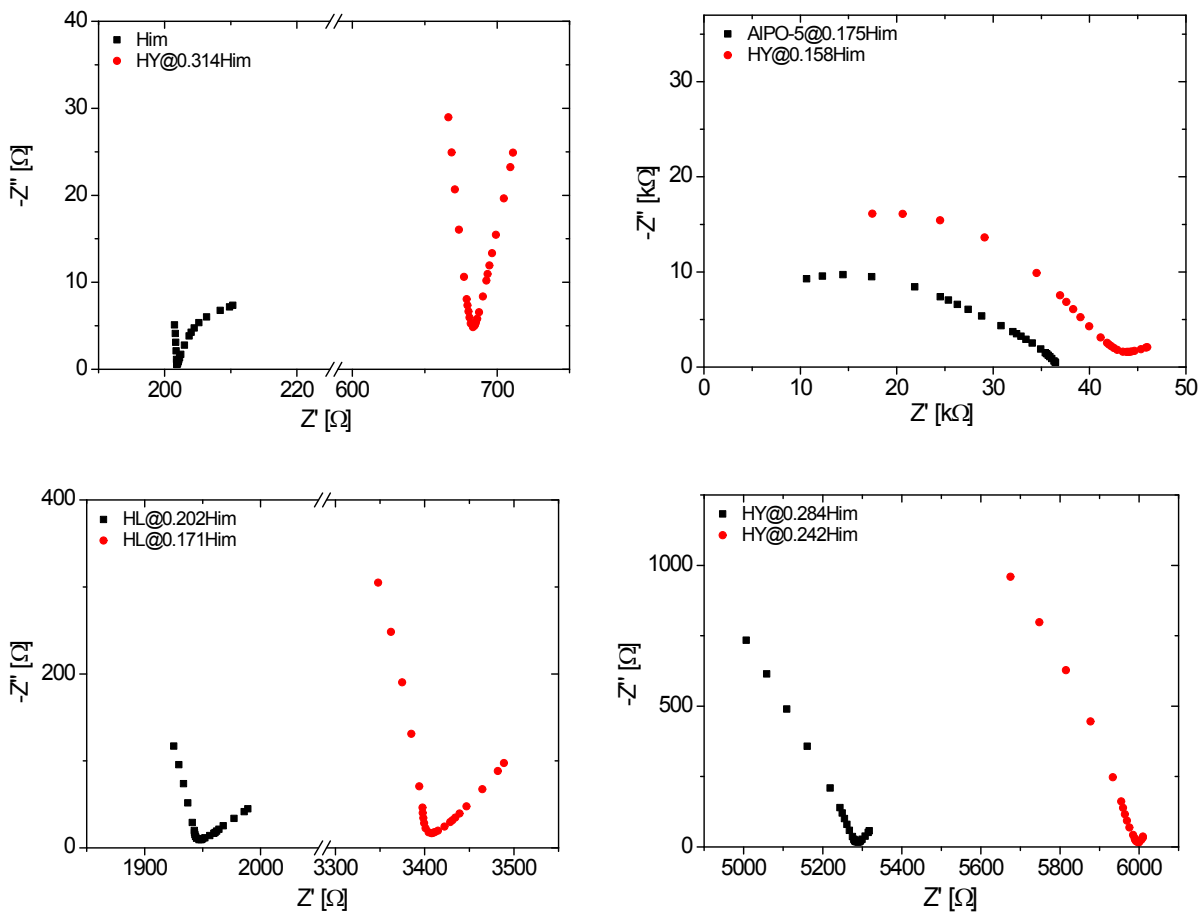


Fig. S4. The Nyquist diagrams for indicated samples at 393 K.



## Conductivity measurement results

Table S3. Conductivity properties of indicated samples.

| HY@Him loading<br>(mass fraction)* | Him density<br>in the matrix<br>[g/cm <sup>3</sup> ]                                      | Him density in<br>acc. space<br>[g/cm <sup>3</sup> ] | Conductivity [S/cm]   |                        | Activation energy [eV]<br>for cooling modes |                  |
|------------------------------------|---|--|-----------------------|------------------------|---|------------------|
|                                    |   |  | 393K                  | 303K                   |   |                  |
| @0.314Him                          | 0.608   | 1.180  | 2.55x10 <sup>-4</sup> | 1.40 x10 <sup>-7</sup> | 0.24<br>(T>330K)                            | 0.83<br>(T<330K) |
| @0.284Him                          | 0.527   | 1.023  | 4.46x10 <sup>-5</sup> | 5.61x10 <sup>-8</sup>  | 0.60<br>(T>346K)                            | 0.84<br>(T<346K) |
| @0.242Him                          | 0.424   | 0.823  | 3.57x10 <sup>-5</sup> | 3.79x10 <sup>-8</sup>  | 0.76  |                  |
| @0.158Him                          | 0.249   | 0.484  | 2.74x10 <sup>-6</sup> | 7.32x10 <sup>-9</sup>  | 0.68  |                  |
| Him                                | 1.232 g/cm <sup>3</sup> (solid) for T>363K<br>1.023 g/cm <sup>3</sup> (liquid) for T<363K |  | 9.83x10 <sup>-4</sup> | 4.48x10 <sup>-10</sup> | 0.24<br>(T>355K)                            | 1.07<br>(T<355K) |

\* assessed by means of elemental analyses (nitrogen content)

Table S4. Conductivity properties of indicated samples.

| Matrix@Him loading<br>(mass fraction)* | Him density<br>in the matrix<br>[g/cm <sup>3</sup> ]                                      | Him density<br>in acc. space.<br>[g/cm <sup>3</sup> ] | Conductivity [S/cm]   |                        | Activation energy [eV]<br>for cooling modes |                  |
|--|---|---|-----------------------|------------------------|---|------------------|
|  |   |   | 393K                  | 303K                   |   |                  |
| AlPO-5@0.175Him                        | 0.358   | 1.114   | 4.66x10 <sup>-6</sup> | 1.16x10 <sup>-7</sup>  | 0.41  |                  |
| HL@0.202Him                            | 0.422   | 1.189   | 6.57x10 <sup>-5</sup> | 1.15x10 <sup>-6</sup>  | 0.45  |                  |
| HL@0.171Him                            | 0.344   | 0.969   | 4.70x10 <sup>-5</sup> | 4.98x10 <sup>-7</sup>  | 0.50  |                  |
| HY@0.242Him                            | 0.424   | 0.823   | 3.57x10 <sup>-5</sup> | 3.73x10 <sup>-8</sup>  | 0.76  |                  |
| AlPO-LAU@0.138Him                      | 0.287   | 0.934   | -                     | -                      | -   |                  |
| Him                                    | 1.232 g/cm <sup>3</sup> (solid) for T>363K<br>1.023 g/cm <sup>3</sup> (liquid) for T<363K |   | 9.83x10 <sup>-4</sup> | 4.48x10 <sup>-10</sup> | 0.24<br>(T>355K)                            | 1.07<br>(T<355K) |

\* assessed by means of elemental analyses (nitrogen content)

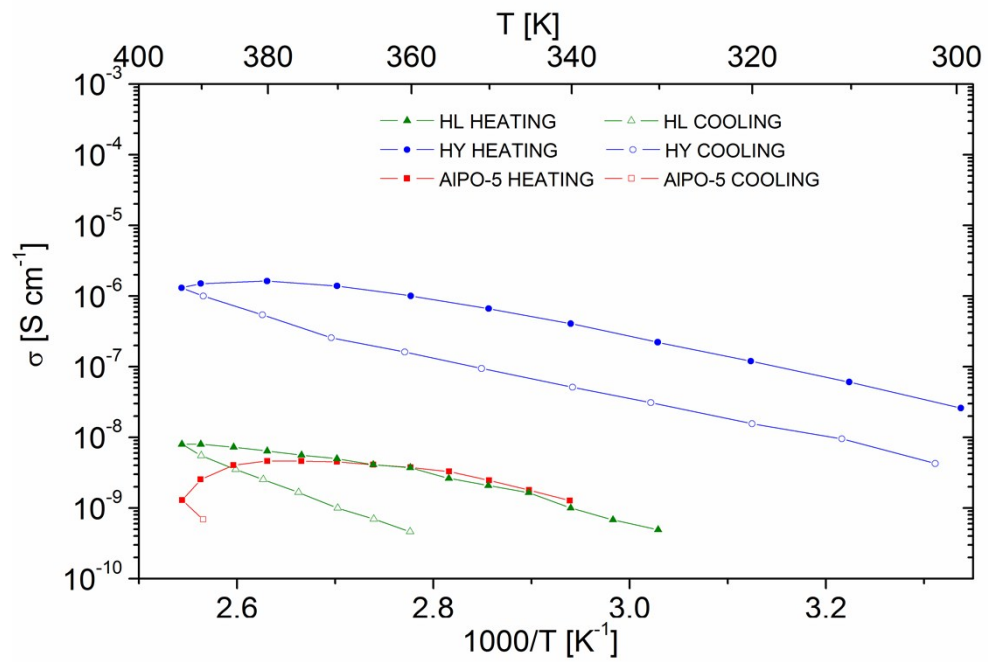
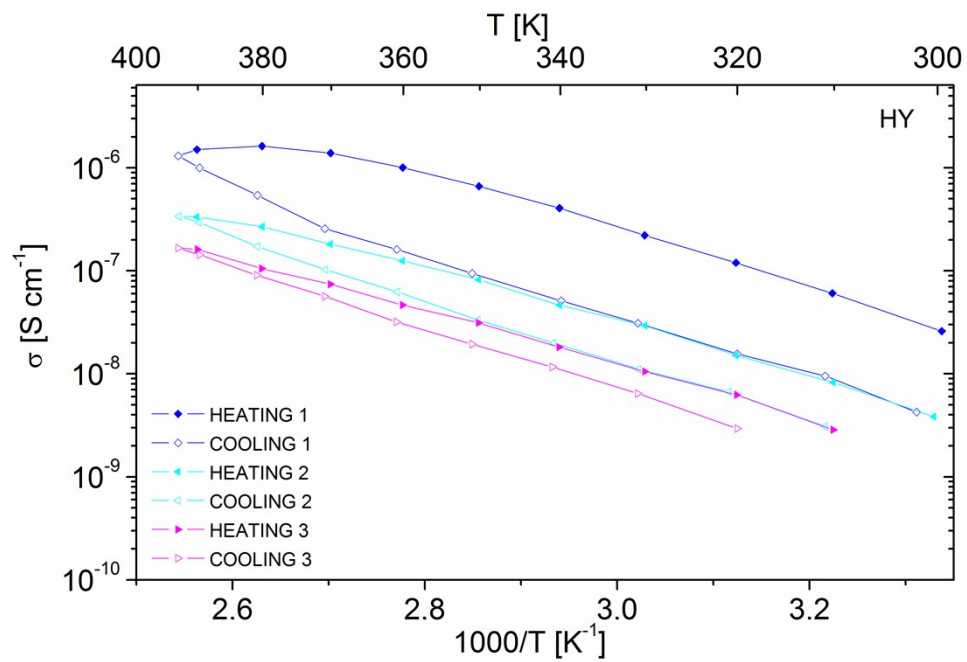


Fig. S5. Correlation between the proton conductivity and temperature for selected lone matrices in heating and cooling mode.

a)



b)

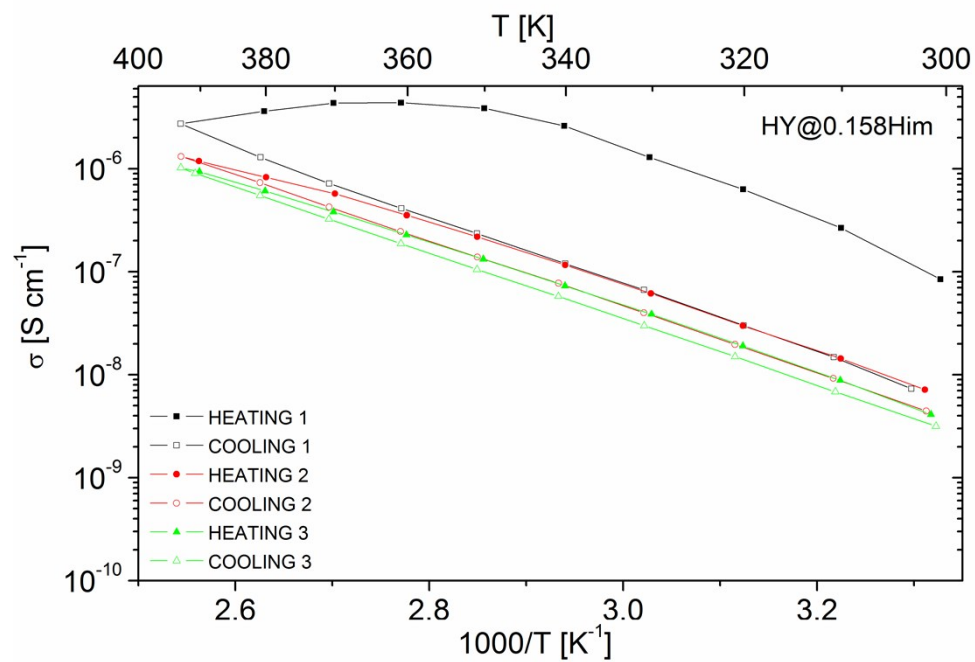


Fig. S6. Proton conductivity of zeolite HY (a) and composite HY@0.158Him (b) as a function of temperature. The cycles (heating/cooling) for both samples were conducted subsequently one after another.

## References:

- 1 S.T. Wilson, B.M. Lok, E.M. Flanigen, U.S. Patent 4,310,440, 1982.
- 2 H. Schulze, U. S. Patent 3,715,365, 1973; D. Heinrich, *Annalen der Chemie und Pharmazie*, 1858, 199.
- 3 <http://www.iza-structure.org/databases/>